Chapter 22

Design of an Electrostatic Ion-Extractor for Laser Isotope Separation Method

- *B. Jana & B. Dikshit*

22.1 Introduction

Atomic Vapor Laser Isotope Separation (LIS) process is a promising technology in separation of desired isotopes having applications in medical science and industry [165]. It consists of several processes like evaporation of vapors and formation of a collimated atomic vapor column, ionization of the targeted isotope through multistep resonant photoionization technique by incident of laser pulses onto the vapor column and collection of photoions on a product collector plate [240]. To get a highly-enriched product, the photoions need to be extracted efficiently and collected at low kinetic energy to a desired location with a minimal contamination by non-selective neutral vapors. Thus, the ion extraction process plays an important role in laser isotope separation method. An efficient electrostatic ion-extractor is designed using plate-grid-grid-plate geometry where the product collector plate is located quite far away from the atomic vapor column. It significantly reduces the non-selective pick-ups resulting in high enrichment of targeted isotope in the product. Starting with a brief description of transient photoplasma evolution in the electrostatic field, the design philosophy of ion-extractor geometry for highly enriched product and a case study of Ytterbium-176 (Yb-176) photoion extraction process are discussed in below.

22.2 Characteristics of Photoplasma and Its Evolution

Photoplasma has unique characteristics. It is generated in a timescale of nano-sec (i.e. pulse duration of laser ∼10 ns) and it exists for a few tens of microseconds. It has a finite size and shape of either rectangular or cylindrical type depending upon the cross-sectional area of incident laser beams. It is surrounded with the vacuum boundary and has a steep density gradient at its edge. It has a low electron temperature of ∼0.1-0.5 eV and the ions' temperature is nearly zero. The charge species are weakly coupled. The collisions of charge species with the neutral background are negligible. Figure 22.1 shows the list of

process through which the photoplasma decays in the electrostatic field [241]. Since the photoplasma is generated inside the atomic vapor column, it has a bulk motion along the vapor propagation direction. Initially the plasma electrons have more kinetic energy than that of photoions. They tend to run away from the plasma volume.

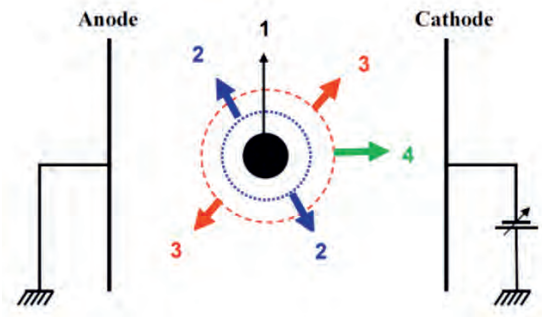

Figure 22.1: List of processes in decay of photoplasma: 1 - Bulk motion, 2 - Ambipolar diffusion, 3 - Coulomb repulsion, and 4 - Child-Langmuir flux.

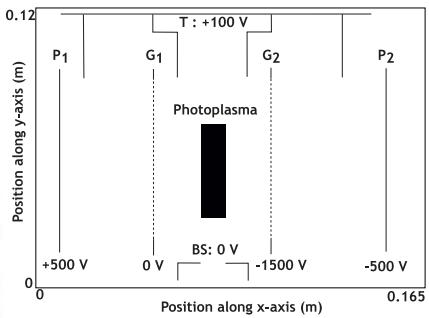

Figure 22.2: Schematic of ion-extractor geometry along with various voltages: P_1 - anode, G_1 & G_2 - grids, P_2 - collector, BS - bottom slit, and T - tail collector.

The positive charge inside the plasma creates a space charged electric field which pulls back the electrons towards the plasma volume. Because of their inertia, the electrons show an oscillatory behaviour in the background of positive ions. The same field also accelerates the cold photoions. The ions defuse from the high density region to the low density region. The plasma expands in the radial direction and the process is called ambipolar diffusion. When an external electrostatic field is applied, a fraction of electrons escape from the plasma as an initial response. The unbalanced positive charges make repulsions among themselves and the plasma expands in the radial direction due to Coulomb repulsion. During its evolution of photoplasma, within a few cycles of plasma electron oscillation, a sheath of electrons is formed between the space of anode plate and plasma boundary. The finite-sized plasma is polarized in such a way that the internal field shields the applied electric field inside the plasma volume. So the entire potential drops between the plasma edge and cathode plate. Towards the cathode plate, the ions move and form an ion sheath between the plasma and cathode plate. The ion motion is governed by the space-charge limited Child-Langmuir (CL) flux. It is supplied by the Bohm flux at the boundary of plasma-ion sheath. With time, the density of plasma decreases and it decreases the Bohm flux. The plasma sheath boundary moves accordingly towards the plasma region in order to balance the Child-Langmuir flux [210]. Towards the anode plate, the finite-sized plasma also expands due to ambipolar diffusion. As the density further decreases with time, the plasma (i.e. collections of charge particles) is unable to shield the external potential and it behaves like single charge particle. Thus, the photoplasma passes through different transient stages while it evolves in the electric field.

The neutral vapors pass through a series of collimators and enter into the laser-atom interaction region. They form a well collimated atomic vapor column. The neutral atom density at the interaction regions affects the process of resonant charge exchange between selectively ionized photoions and neutral atoms of non-selected isotopes. In case of (say) Yb-176 isotope separation process, the typical value of charge exchange cross section (σ_{ex}) is $\sim 2 \times 10^{-14} cm^2$. This leads to a collision probability of less than 1% at neutral atom density of $\sim 2 \times 10^{11} cm^{-3}$. In this neutral atom density regime, the probability of atom-atom collision is also negligible. Thus, this makes the non-selective neutral vapor deposition on the product collector plate negligible. With a given ionization yield of ~20% for Yb-176 targeted

isotope with natural abundance of ∼13%, the typical photoplasma density is $\sim 5 \times 10^9$ cm^{-3}. Since the collisions of charge species i.e. electrons and photoions with the neutral atoms at the background are negligible, the photoplasma evolves as fully ionized plasma though it is produced inside the vapor column. The photoions are extracted from the plasma by applying the electrostatic field. The efficiency of ion-extraction process depends on various parameters such as plasma density, applied electric field, plasma dimension (width) and electron temperature etc.

22.3 Design Philosophy: An Efficient Electrostatic Ion-extractor

A conventional structure of electrostatic ion-extractor is formed by placing two parallel plates on both side of the photoplasma. The photoions are extracted efficiently and collected on the cathode plate by applying a large negative potential on it and keeping a small gap between the plasma and cathode plate. Though a major fraction of photoions is collected on the cathode plate but a significant fraction of photoions reaches on the anode plate due to the ambipolar diffusion. In the above parallel plate geometry, the product collector plate i.e. cathode plate is placed at a close distance from the atomic vapor column. A significant amount of non-selective vapors also deposits on the collector plate. It limits the high enrichment of the product. In addition, the kinetic energy of photoions hitting the collector plate is also large (few keV) which causes the sputtering loss of enriched product from the collector plate. It reduces the overall quantity of the product. Thus, it is required to design an efficient ion-extractor with very less sputtering loss and minimum non-selective scattering to get a highly-enriched product of significant quantity. To achieve this objective, recently a new ion-extractor geometry has been proposed using plate-grid-plasma-grid-plate configuration as shown in Fig. 22.2 and the details of which has been explained in [212]. In the new configuration, two highly transparent grids G_1 and G_2 are symmetrically placed on both side of the photoplasma. After the grid structure, two plates P_1 and P_2 are located asymmetrically at different distances from the grid G_1 and G_2 respectively. The product collector plate P_2 is situated at the farthest distance to minimize the non-selective vapors on it. The cross sectional view of extractor geometry is shown in Fig. 22.2. A bottom slit with a narrow rectangular aperture is used to make a well collimated atomic vapor column at the interaction region. The neutral vapors deposit on the tail. Even at the temperature of ∼150 °C, the deposited Yb vapors can re-evaporate from the tail and it increases the possibility of non-selective deposit on the product collector. So, the tail structure is modified to reduce the vapor deposition of re-evaporated vapors on the product collector plate P_2. This ion extraction/collection geometry has four electrodes. The potentials on them can be changed independently. The selection of applied potentials on different electrodes like P_1, G_1, G_2 and P_2 plays a crucial role in the ion extraction process in the new geometry. It shows three-fold advantages. Firstly, a large negative potential applied on the grid G_2 extracts the significant fractions of ions from the photoplasma. They pass through the highly transparent grid G_2 and move towards the product collector plate P_2. Secondly, a positive potential is applied on the repeller plate P_1, it repels the ions that pass through the grid G_1 towards the photoplasma. Thus, it reduces the loss of ions which move towards the repeller plate P_1 due to ambipolar diffusion. Thirdly, a less negative potential is used on the product collector plate P_2 which reduces the kinetic energy of photo-ions resulting in soft landing of ions on the collector plate. As a result, the sputtering loss of product decreases. Therefore, above ion-extractor geometry with appropriate voltage configuration provides the highly-enriched product of targeted isotope in laser isotope separation process.

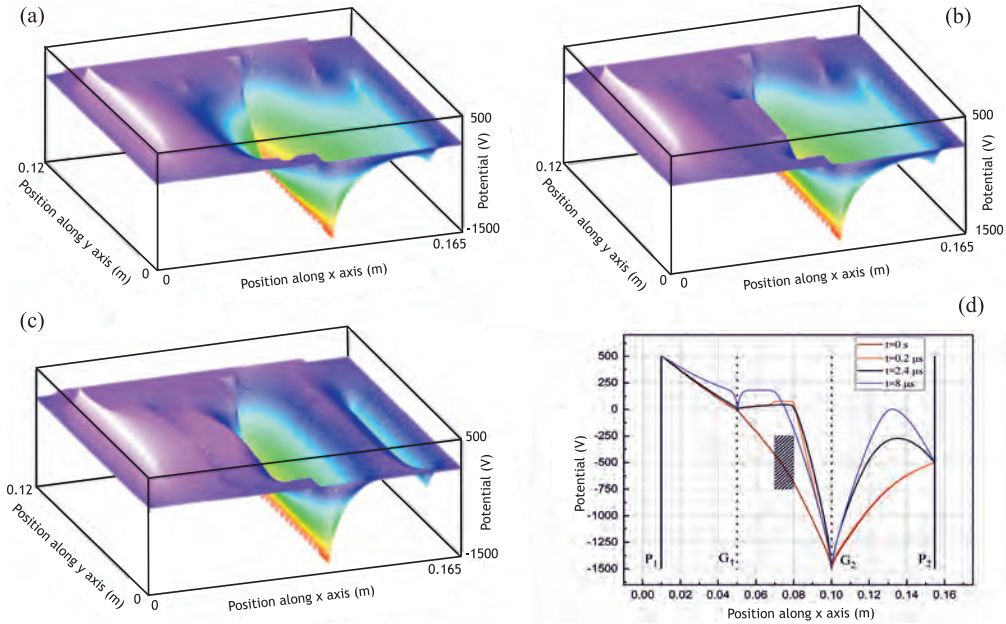

Figure 22.3: Potential distribution over the computational area at time t = 0 s (a), t = 0.2 μs (b), t = 2.4 μs (c), and (d) Comparison of central line potential distribution along X axis.

22.4 2D XOOPIC Code

The transient evolution of the finite sized photoplasma at a cross sectional plane of above ion-extractor geometry is simulated using 2-D XOOPIC code. The XOOPIC (X-windows based Object Oriented Particle-In-Cell) is a two dimensional relativistic electromagnetic PIC code [242]. It was developed by the plasma theory and simulation group of Michigan State University, USA. It is a versatile code used by the plasma physicists in understanding the kinetics of plasma evolutions. The basic structure of PIC simulation is discussed in brief. In the PIC simulation, the plasma is replaced by less number of positive and negative charged macro particles. Each macro-particle carries more mass and charge than that of individual ion and electron with having the same charge to mass ratio of individual one. The motion of macro-particles is simulated at a 2D plane known as computational box. Here it is a rectangular area and the 2D XY coordinate system is used to represent it. The rectangular area is discretized into spatial meshes (or grid points). At the grid points, the charge density is calculated from the particle's positions. To get the potentials at different grid points, the Poisson's equation is solved. The forces on the macro-particles are calculated from the Lorentz equation. The velocity and position of the particles are estimated by solving Newton's equation of motion. The iterative execution of the above steps self-consistently calculates the electric field due to both space charge field and external electric field. It describes the motion of macro-particles in the computational box. During their motion, when the macro-particles cross the boundary or electrode, they are lost from the computational box. Various input parameters required to run the 2D-XOOPIC code are listed in table 22.1.

Table 22.1: List of input parameters for simulation of Yb-176 photoplasma by XOOPIC code.

Input Parameters	**Values**
Element	Ytterbium
Mass of ions	176 amu
Plasma density ($n_e = n_i$)	5.0 x10^9 cm^{-3}
Electron temperature ($T_e \sim \Delta E$)	0.24 eV
Ion temperature (T_i)	~0 eV
Plasma dimension	1 cm x 4 cm
Dimension of computational area	16.5 cm x 12 cm
Separation between grid points (dx)	~0.064 cm
Separation between grid points (dy)	~0.046 cm
Time step	5.0x10^{-11}s
No of positive super particles	1.0x10^5
No of negative super particles	1.0x10^5
Potential applied on P_1, G_1, G_2 and P_2 plates	+500 V, 0 V, -1500V, & -500 V respectively

22.5 Results and Discussion

A finite-sized Yb photoplasma of dimension 1 cm x 4 cm having plasma density 5x10^9 cm^{-3} is evolved in the above electrostatic ion-extractor. The potential applied on the electrode P_1, G_1, G_2 and P_2 are +500 V, 0 V, -1500 V and -500 V respectively. The bottom slit is kept at 0 V and the tail structure is biased at +100 V. A case study of Yb-176 photoplasma evolution is carried out. Figure 22.3 shows the potential distribution over the computational area at times (a) t = 0 s, (b) t = 0.2 μs and (c) t = 8 μs. The central line potential along X axis at different times is compared in Fig. 22.3d. It is observed that the potential distribution gets modified from its initial distribution as shown in Fig. 22.3a. The plasma attains a potential which is slightly positive than the potential applied on the grid G_1. The electrons move towards the grid G_1 and the finite-sized plasma is polarised to shield the applied external field inside the plasma volume. The applied potential drops between the plasma edge and grid G_2. The motion of macro-particles is governed by the field of both externally applied electric field and self generated ambipolar field in the plasma. The plasma particles evolve through various quasi-steady stages with time. The Fig. 22.4 shows the evolution of positive macro-particles. The initial positions of positive macro-particles are represented in Fig. 22.4a. The photoions move under the external field towards the grid G_2 and form an ion sheath in between the plasma and grid G_2 as shown in Fig. 22.4b. Because of the highly transparent grid G_2, the ions pass through the grid G_2. They further move towards the plate P_2 and are collected on the product collector plate P_2. This is shown in Fig. 22.4c. The presence of photoions also changes the potential distribution as shown in Fig. 22.3d at time t = 2.4 μs. The Fig. 22.4d represents the expansion of plasma ions towards the grid G_1 due to ambipolar diffusion. They are repelled by the positive potential applied on the plate P_1. During its evolution, the ions are accelerated between the plasma and grid G_2 while approaching the grid G_2 and decelerate between the grid G_2 and collector plate P_2. It creates a bunching of positive ions in the space. So towards the collector plate, as

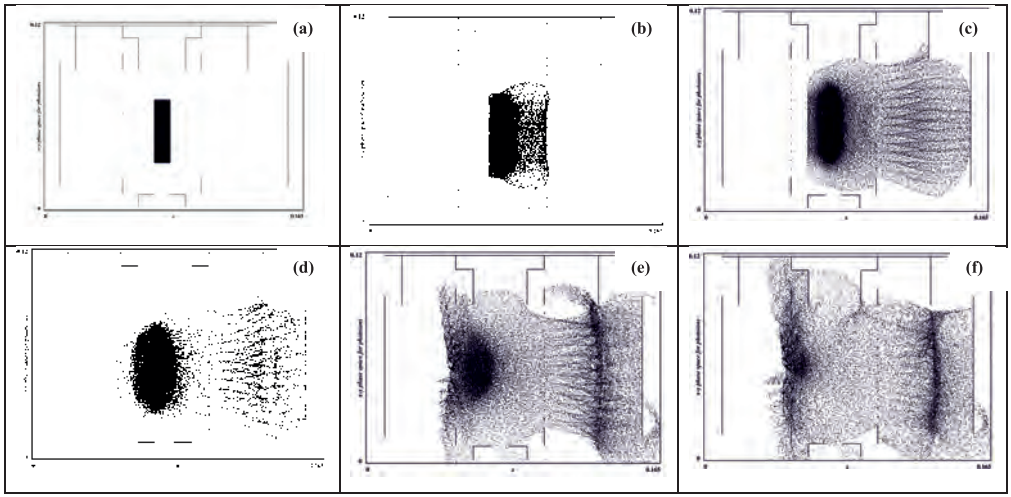

Figure 22.4: Evolution of positive super particles with time, (a) t = 0 s, (b) Formation of ion sheath, t = 1 μs, (c) Ions reaching to P_2, t = 2.4 μs, (d) Plasma expansion towards G_1, t = 4 μs, (e) Bunching of ions between G_2 and P_2, t = 8 μs, (f) Coulomb repulsion, t = 10.8 μs.

their velocity decreases, the plasma ion density increases due to the conservation of ion flux. The accumulation of positive charge creates a space charge field which modifies the potential distribution between grid G_2 and plate P_2 as shown in Fig. 22.3c at time t = 8 μs. The positive ion bunch expands in radial direction due to coulomb repulsion. Though a major fraction of ions are collected on the plate P_2 but many of them also bounce back towards the grid G_2. The ions' motion shows an oscillatory motion across the grid G_2. The photoions are collected on the plate P_2 and generate an ion current pulse. The typical shape of ion current pulse simulated from the 2D-XOOPIC code is shown in Fig. 22.5. It clearly indicates that the photoions are collected within a time of ∼22 μs. The ion collection time mainly depends on the plasma density, potentials configurations. The area of ion-current pulse on the plate P_2 estimates the total ions reached on the collector plate. The ion collection efficiency is calculated from the ratio of photoions landed on the collector plate P_2 to the initial number of photoions considered for the plasma simulations. For the above potential configuration, the estimated ion-collection efficiency is ∼62%. Though it increases with the potential applied on the plate P_2, but at the same time it increases the kinetic energy of photoions hitting on the collector plate. The Fig. 22.6 shows the energy distribution of photoions collected on the plate P_2 biased at -500 V. The photoions have an average energy of ∼600 eV. It is observed that the energy of ions is gained more than 500 eV. This is may be due to the space charge internal field created by the positive ion bunch. At the above low kinetic energy of photoions, the contribution of sputtering loss from the product collector plate is negligible. It is also noted that at higher plasma density a very less fraction ($< 0.5\%$) of ions reach to the repeller plate P_1 though it is biased at +500 V. It is because of space charge internal field due to the ion bunch which modify the potential distribution during the evolution of photoplasma. In the recent experiments of targeted Yb-176 isotope separation, the measured scattering fraction of non-selective vapors on the plate P_2 is less than 0.1% of that entered into the interaction region. The achieved product quality is more than 97% with product quantity of nearly 3 mg per hour from the plasma column length of ∼15 cm with the above ion-extractor geometry and voltage configuration.

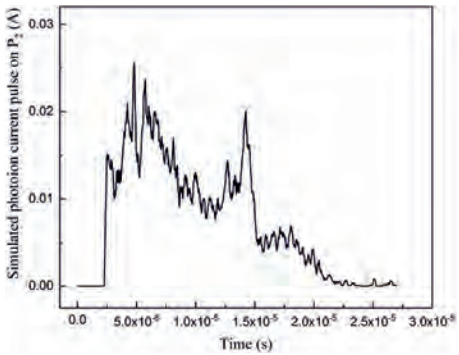

Figure 22.5: The typical pulse shape of photoion current on the collector plate obtained from XOOPIC code.

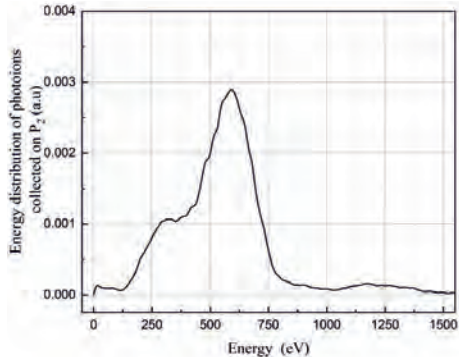

Figure 22.6: Energy distribution of photoions hitting the product collector plate P_2 biased at -500 V.

22.6 Conclusions

A new electrostatic ion-extractor has been designed with plate-grid-plasma-grid-plate configuration to get a highly-enriched product of targeted isotope in laser isotope separation process. The transient evolution of Yb-176 photoplasma has been carried out in the ion-extractor. A less negative potential of ∼-500 V is applied on the collector plate for soft-landing of ions to avoid the sputtering loss of the enriched product from the collector plate. The estimated ion collection efficiency is ∼62% with the potential configuration of +500 V, 0 V, -1500 V and -500 V applied on P_1, G_1, G_2 and P_2. The ion collection efficiency varies with the applied potential configuration and the plasma density which may be optimized for the actual geometry.